5

Integration of 5G Sub-6 GHz and mm-Wave Higher-Order MIMO Antenna for Smartphone's Back Covers

*In this chapter, an extremely low-profile/compact MIMO system is proposed by utilizing the dual antenna for 5G sub-6 GHz and mm-wave applications. The antennas are integrated on a centrally located square-shaped slot-loaded octagon-shaped substrate. The identical dual antenna elements with the same orientation are orthogonally placed on an octagon-shaped substrate from the outer side, creating an 8-element MIMO antenna for 5G sub-6 GHz application. From the inner side of the same substrate, a 1×4 array-based antenna is orthogonally placed in front of the remaining side of the octagon, forming a 4-element MIMO antenna for 5G mm-wave application. The stubs are connected to shared ground plane to reduce the coupling between antenna elements. The MIMO system provides dual -6 dB impedance bandwidth of ($S_{ij} \in i=j$, 1 to 8) 4.0-5.6 GHz and ($S_{ij} \in i=j$, 9 to 12) 24.25-29.5 GHz. It has a minimum isolation ($S_{ij} \in i \neq j$) value of 12 dB and 22 dB, respectively. Due to 0.508 mm low-profile, antenna is integrated within the back cover of smartphones, thereby inside device volume will reduce. The measured and simulated results are found in close agreement those confirming that the proposed MIMO system may be a suitable candidate for 5Gsmartphones **

*Parts of this chapter have been published: Arun Kumar Saurabh and M. K. Meshram, "Integration of sub-6 GHz and mm-wave antenna for higher-order 5G-MIMO system," *IEEE Transactions on Circuits and systems II: Express Briefs,* 2022, DOI: 10.1109/TCASII.2022.3197598.

5.1 Introduction

The needs of high-speed data with low latency day by day are increasing. The fifth-generation (5G) communication is attracting more attention after 4G, as it is ensured to overcome the restriction of current wireless communication [118]. In many countries, 5G NR (New Radio) wireless communication has been focused on the spectrum band n77/n78/n79 (3.3-4.2 GHz/3.3-3.8 GHz/4.4-5.0 GHz) below sub-6 GHz [140] because it provides a larger coverage area having lesser propagation losses. On the other hand, millimeter-wave spectrum n257/n258 (26.5-29.5 GHz/24.25-27.5 GHz) [141] is also demanding in short-range coverage areas with considerable losses is promised to increase the data capacity and connections throughput with other hosts. Several antenna designs are available in the recent literature for 5G applications. However, mostly higher-order MIMO designs only cover the 5G sub-6 GHz band [86], [94], [112], [142]-[152] and some cover the 5G mm-wave band only [82], [153]-[157]. To the best of the authors' knowledge, very few MIMO antennas are available that integrate 5G sub-6 GHz and mm-wave band simultaneously on the same board [89]-[90], [158]. Therefore, the integration of both bands is a more challenging task for the researchers. Integrating multiple antennas into compact/low-profile/portable user devices are essential for extremely high data rates with throughput. Still, the area available to integrate the multiple antenna elements inside the devices is limited. To overcome this issue, the ultra low-profile multiple antennas have been installed inside/cavity-loaded back cover of the low-profile user devices. In [112], [150]-[152], the total thickness of the antenna has been proposed as 1 mm, 0.787 mm, 1.2 mm, and 0.97 mm, respectively for a low-profile antenna. The antenna thickness also depends on the thickness of the substrate (t), and it should be very thin for low-profile because the power leakage issue can quickly occur in the thick substrate-based antennas. As a result, surface waves are excited, and it is the function of dielectric

constant (ε_r) and substrate thickness (t). To neglect the influence of the surface wave propagation, substrate thickness should follow the given criterion [159]. Therefore, a compact/ultra-low-profile higher-order MIMO antenna inside the device's back cover along with 5G sub-6 GHz and the mm-wave spectrum is the best alternative to address the aforementioned issue.

In [142]-[149], the 8-element MIMO antennas have been proposed for 5G (n77/n78/n79 of sub-6 GHz) smartphones, where the antenna elements and antenna pairs integrated on the side edge of metal-rimmed terminals of the smartphone PCBs (printed circuit boards). In [86], a set of four inverted-L and top-hat-shaped monopole antennas were designed on the top and bottom side of the common ground PCB. Dual-polarized square-ring slot radiators etched on the PCB fed through two microstrip lines form an 8-element MIMO antenna [94]. A new antenna designing approach for 5G smartphone was proclaimed, where the extremely low-profile MIMO antennas were installed inside cavity loaded dielectric back cover, printed on the substrate of the dielectric back cover, and also integrated antenna's board as a smartphone back cover, i.e., the grounded coplanar waveguide (GCPW) fed 4-port open slot antennas were integrated inside the cavity loaded dielectric back cover [112], wideband eight-element microstrip antennas directly fed by the coaxial probes [150] and dual-polarized eight-element microstrip antennas fed by the differential feed [151] were printed on the substrate of the smartphone dielectric back cover, and the board of the four pairs inverted-F antennas configures on the artificial magnetic conductor (AMC) ground were integrated as a smartphone back cover [152], respectively.

Some antenna configurations have been reported based on the array concept for 5G (mm-wave band). Two 1×8 array antennas placed 180° out of phase form a 2-port 16-element (2×8 array) array antenna [153]. A 1×4 antenna array based on substrate

integrated cavity (SIC) was mirrored around the axis creates a 1-port 8-element (1×8 array) antenna array [154]. In [155], a differentially fed dielectric resonator-based 1×2 array was utilized to form a 2-port 4-element (2×2 array) antenna with dual polarization characteristics. A combination of (parasitic, shorting, and driven) patches was fed by the differentially feeding technique used to create a 2×2 array with bandpass filtering characteristics [156]. In [157], two rectangular dielectric resonator-based 2-element MIMO antenna was presented to improve the isolation for the operating range 27.25-28.59 GHz. A 4-element optically transparent MIMO antenna was designed to cover 24.10-27.18 GHz [82]. Further, a dual-band 2-element MIMO antenna was integrated with a 1×4 array for Sub-6 GHz (2.45-2.85 GHz and 3.18-3.68 GHz) and mm-wave band (25-30 GHz) [89]. In [90], a common aperture integrated antenna system for 5G sub-6 GHz and mm-wave application. Integration of frequency reconfigurable 8-element MIMO for 5G sub-6 GHz and mm-wave band by placing antenna element on the sides of PCB [158]. However, based on the above-discussed literature, a novel approach is required, which can integrate a higher-order MIMO antenna for 5G sub-6 GHz and mm-wave application on the same board and can also be utilized in ultra-low-profile user's devices.

In this chapter, integration of an extremely low-profile/compact 8-element MIMO antenna and 1×4 array-based 4-element MIMO antenna on a common aperture are proposed for 5G spectrum band n79/n257/n258. It has ensured a low coupling between a pair of elements along with satisfactory diversity performances. Further, the proposed MIMO antenna is installed inside the cavity-loaded dielectric back cover of the smartphones. Its results are found almost close to free-space MIMO antenna without compromising any aspect that is the novelty of the MIMO system. The complete details of the proposed MIMO system are discussed in the following sections.

5.2 Details of 5G-MIMO Antenna

The configuration of the proposed 5G-MIMO antenna with shape parameters is illustrated in Fig. 5.1(a) and Fig. 5.1(b) shows the zoomed view of 1×4 array with dimension parameters. The prototype is fabricated on a centrally located square-shaped slot-loaded octagon-shaped cross-section area of 3706.69 mm^2 [(L_A×L_A)–(1/2×L_R×L_R)4–(L_{g3}×L_{g3})] or about 0.6589 λ_0^2, (where λ_0 is the free-space wavelength at the lowest frequency of the 4.0-5.6 GHz band) of Roger 5880 substrate (ε_r=2.2, *tan* δ=0.002, thickness t=0.508 mm).

5.2.1 8-Element MIMO Antenna Structure

The geometry of the 8-element MIMO antenna is etched on a centrally located square-shaped slot-loaded octagon-shaped substrate board. To achieve the lowest operating frequency of the n79 spectrum on that area is the basic need of the proposed 5G-MIMO antenna. Therefore, the preliminary design of the MIMO antenna element starts by selecting a simple planar trapezium-shaped monopole element fed through the microstrip line and their dimensions optimized to achieve the n79 spectrum.

The monopole antenna element of the proposed 8-element MIMO antenna consists of the modified trapezium-shaped patch with the rectangular ground plane, which is fed through 50 Ω microstrip line feed from the outer side on the octagon-shaped substrate. The two identical monopole antennas are placed in the same orientation on the substrate cross-section area of 19×35 mm^2, and the minimum edge-to-edge distance kept between them is less than $\lambda_0/8$ (6 mm = 0.08λ_0). A stub is connected with antenna's ground plane to achieve better impedance matching and low correlation between same oriented elements simultaneously. It achieved the sub-6 GHz band of n79 with high isolation, as shown Fig. 5.2(a). Next, these are orthogonally symmetrically arranged on the same substrate from the outer side, forming an eight-element MIMO antenna. On the bottom side of the substrate, the discrete rectangular ground planes are interconnected through

the connecting strips to make a shared ground plane. Further, a combination of ground stubs is interconnected with the common ground plane between a pair of the corner elements (as element-1 and element-8) to reduce the mutual coupling. Finally, the proposed 8-element MIMO antenna is successfully obtained satisfactory performances for the 5G sub-6 GHz (n79) band going through the optimized design evaluation and optimized design dimensions parameters.

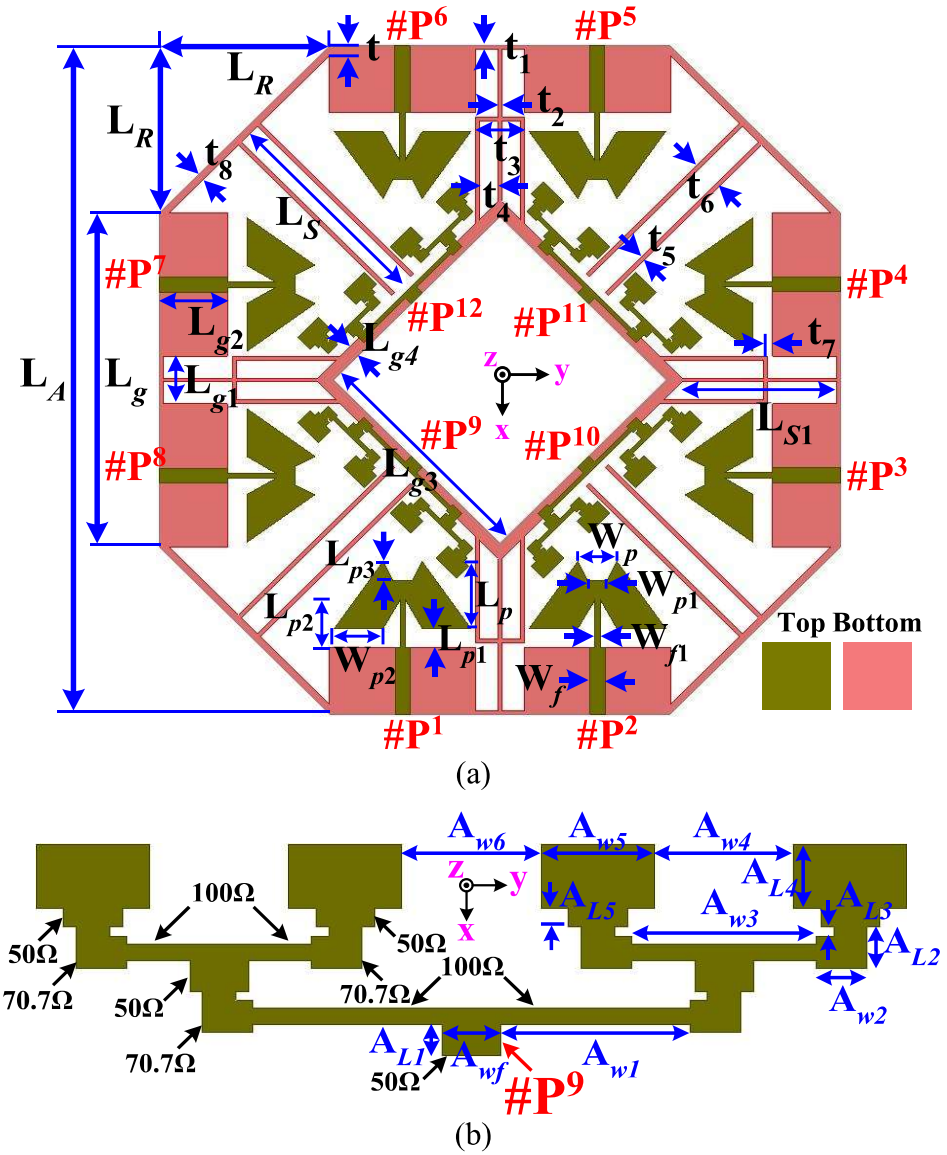

(a)

(b)

Fig. 5.1: The MIMO antenna (a) configuration with shape parameters and (b) zoomed view of 1×4 array.

Dimensions (*in mm*): L_A=70, L_R=17.5, L_g=35, L_{g1}=5, L_{g2}=7, L_{g3}=24.1, L_{g4}=1.29, t=1, t_1, t_2=0.4, t_3=5, t_4=1.9, t_5=0.4, t_6=3.13, t_7=0.5, t_8=0.707, L_S=22.27, L_{S1}=15.93, L_p=7, L_{p1}=2, L_{p2}=5, L_{p3}=2, W_p=4, W_{p1}=2, W_{p2}=5, W_f=1.56, W_{f1}=0.52, A_{L1}=0.85, A_{L2}=1.12, A_{L3}=0.24, A_{L4}=1.75, A_{L5}=0.5, A_{wf}=1.56, A_{w1}=5.02, A_{w2}=1.34, A_{w3}=4.9, A_{w4}=3.7, A_{w5}=3, A_{w6}=3.7.

5.2.2 1×4 Array Based 4-Element MIMO Antenna Structure

The preliminary design of the 1×4 array-based MIMO antenna element starts by selecting a rectangular monopole element fed through the microstrip line and dimensions are optimized to achieve the n257/n258 spectrum. Further, a simple rectangular 1×4 array antenna with a partial ground plane is configured on the substrate cross-section area of 10×24.1 mm^2 for the same frequency band, which is fed through a 50 Ω corporate feed network. Each 50 Ω feed line consist of two parallel 100 Ω, 70.7 Ω transmission line, and four rectangular patches are terminated with four 50 Ω feed line, as shown in Fig. 5.1(b). It provides the mm-wave spectrum of n257/n258, as shown in Fig. 5.2(b). Furthermore, a 1×4 array antenna is symmetrically orthogonally placed from the inner side on the top of the same substrate, creating a 1×4 array-based 4-element MIMO antenna. The array elements are oriented in front of the octagon-shaped substrate's remaining sides, as shown in Fig. 5.1(a). Their partial rectangular ground planes are connected with the stubs-loaded ground plane of the 8-element MIMO antenna to make a complete shared ground plane. The beauty of the design is that any decoupling structures are not required between the array elements. The same ground stubs are also utilized as a decoupling structure to reduce the coupling in the array-based MIMO antenna. Finally, a 1×4 array-based 4-element MIMO antenna is ensured satisfactory performances without compromising any aspect going through the optimized dimensions parameters for the mm-wave spectrum.

5.2.3 Higher-Order 5G-MIMO Antenna Configuration

As a result, a higher-order 5G-MIMO system is proposed by integrating both MIMO antennas simultaneously (8-element MIMO antenna for 5G sub-6 GHz and 1×4 array-based 4-element MIMO antenna for 5G mm-wave). In the proposed 5G-MIMO system, the antenna elements are extremely closely placed, i.e., element-1 and element-9. The edge-to-edge distance between element-1 and element-9 is almost close to $\lambda_0/64$ (1.421

mm or 0.018λ_0, λ_0 at 4.0 GHz). To achieve good isolation between extremely closely spaced elements is one of the novelties in the presented proposal. The 5G-MIMO system successfully provides dual-band -6 dB simulated impedance bandwidth of 4.0-5.6 GHz ($S_{ij} \in i=j$, *1* to *8*) and 24.25-29.5 GHz ($S_{ij} \in i=j$, *9* to *12*) simultaneously. It has minimum isolation ($S_{ij} \in i \neq j$, *1* to *12* and *9* to *12*) values of 12 dB and 22 dB in the respective frequency band. The obtained results show the MIMO system's capability for 5G application-oriented compact/low-profile user's devices.

5.2.4 Effect of Decoupling Structures on Common Ground

The current distribution plot on the surface of the ground plane along with antenna elements is presented to analyze the effectiveness of decoupling structures at frequency 4.9 GHz when element-1 (#P^1) is kept excited, and the rest of all are kept matched terminated. Fig. 5.3(a) show that the orientation of the coupling current is concentrated to the whole ground with a combination of ground stubs, mainly toward element-3 (#P^3), element-5 (#P^5), element-7 (#P^7), element-9 (#P^9) and element-10 (#P^{10}). As a result, moderate isolation between them is observed in the sub-6 GHz frequency spectrum, better than -12 dB (transmission coefficients $S_{ij} \in i \neq j$). To reduce the correlation, a combination of the ground strip is connected to the common ground and placed between two identical antenna elements, i.e., element-1 (#P^1) and element-2 (#P^2), and element-9 (#P^9) and element-10 (#P^{10}). The orientation of surface current is highly concentrated on the combination of the ground strip, decreasing the coupling current mainly from element-1 (#P^1) to element-2 (#P^2). However, some part of the coupling current still flows from element-1 (#P^1) to element-8 (#P^8), element-9 (#P^9), and element-10 (#P^{10}), and the resulting coupling between element-1 (#P^1) and element-2 (#P^2) is reduced. Another dual I-shaped ground strips are connected to the common ground and placed between two corner antenna elements, i.e., element-1 (#P^1) and element-8 (#P^8) and two patches of the

1×4 array. The orientation of surface current is highly concentrated on dual I-shaped strip and the combination of the ground strips on common ground plane, therefore decreasing the coupling current from element-1 (#P^1) to element-2 (#P^2), element-8 (#P^8), and element-9 (#P^9). As a result, coupling between antenna elements better than -12 dB (coupling coefficients $S_{ij} \in i \neq j$) is obtained in the sub-6 GHz band.

Similarly, at the frequency of 26.5 GHz, element-9 (#P^1) is kept excited, and the rest of all are kept matched terminated. Fig. 5.3(b) shows that the orientation of the coupling current is highly concentrated toward ground connected stubs between element-1 (#P^1) and element-2 (#P^2), element-1 (#P^1) and element-8 (#P^8), element-7 (#P^7) and element-8 (#P^8) due to this low coupling are observed in the mm-wave frequency spectrum, which is better than 22 dB (coupling coefficients $S_{ij} \in i \neq j$).

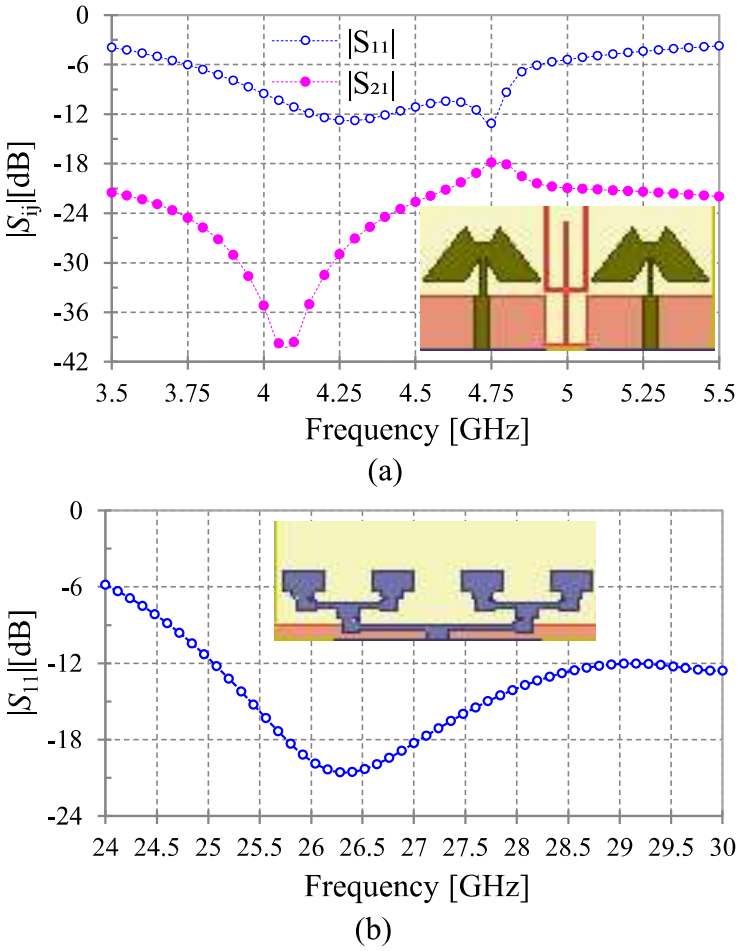

Fig. 5.2: (a) Two-element MIMO antenna configuration corresponding *S*-parameters and (b) 1×4 array configuration corresponding S_{11}-parameter.

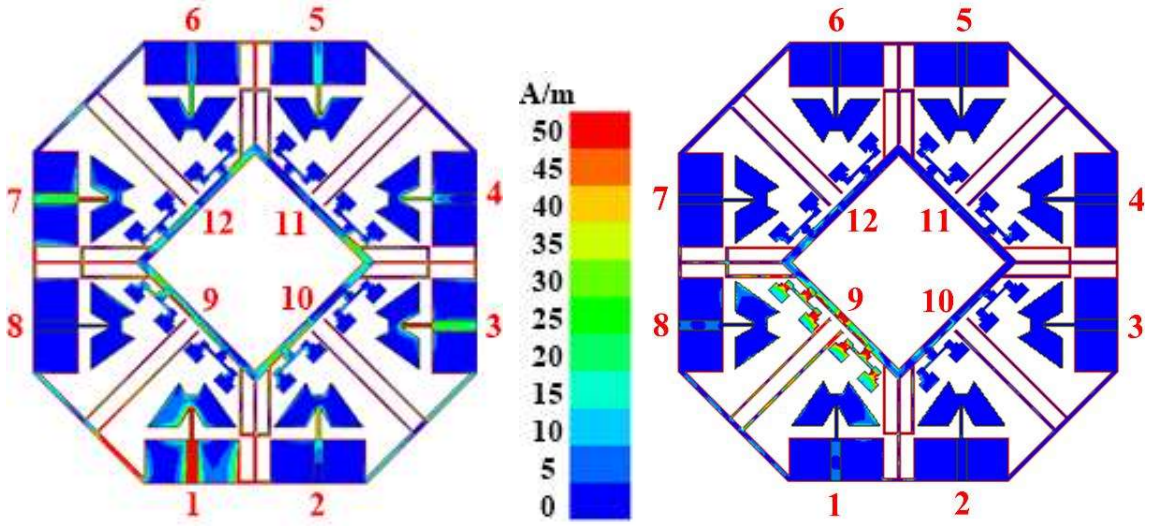

(a) (b)

Fig. 5.3: Surface current distribution on the shared ground (a) element-1 (#P[1]) is kept excited at 4.9 GHz and (b) element-9 (#P[9]) is kept excited at 26.5 GHz, and the rest of the elements are kept matched terminated.

5.3 Results and Discussion

The performances of the proposed higher-order 5G-MIMO system are analyzed in the following sections.

5.3.1 *S*-parameter Performances

The top and bottom views of the prototype are shown in Fig. 5.4(a)-(b). The *S*-parameters results are measured using Keysight FieldFox Microwave Analyzer (model: *N9951A*), as plotted in Fig. 5.4(c)-(d). The proposed 5G-MIMO antenna achieved dual-band -6 dB impedance bandwidth of 4.0-5.6 GHz ($S_{ij} \in i=j$, *1* to *8*) and 24.25-29.5 GHz ($S_{ij} \in i=j$, *9* to *12*). It provides a minimum mutual coupling value of -12 dB and -22 dB ($S_{ij} \in i \neq j$, *1* to *12* and *9* to *12*), respectively, in the respective spectrum. The reflection coefficient S_{11} is only illustrated here because the remaining reflection coefficients $S_{ij} \in i=j$, *2* to *8* are almost identical for the n79 spectrum. Similarly, S_{99} is only shown here for the n257/n258 spectrum, and the rest of the all $S_{ij} \in i=j$, *10* to *12* are almost similar to S_{99}. All coupling coefficients are almost identical to $S_{ij} \in i=1$, $j=2$ to *12,* and $S_{ij} \in i=9$, $j=10$ to *11*. The

inconsistency occurred between the simulated and measured results mainly due to manual tolerances in fabrication, soldering, and testing of the antenna having a non-rigid substrate board, which can be minimized in mass manufacturing at the industry level. The proposed 5G-MIMO antenna successfully secured the measured 5G sub-6 GHz spectrum of n79 with a moderate isolation value. Also, it covered the mm-wave spectrum band of n257/n258 with high isolation and better impedance matching in the n258 spectrum. The obtained results show the MIMO system's capability for 5G application-oriented compact/low-profile user's devices, i.e., smartphones, tablets, etc.

5.3.2 Radiation Performances

Fig. 5.5(a)-(b) show the 2-D radiation patterns (simulated and measured) for element-1 and element-9 of the proposed antenna at 4.81 GHz and 26.5 GHz, respectively. The 2-D radiation patterns are plotted in two principal planes (xz and yz) when one port is excited and the other ports are kept matched terminated. The measured 2-D radiation pattern is plotted at 4.81 GHz, closely matched with simulated having an omnidirectional pattern with good co-to-cross isolation. Similarly, at 26.5 GHz, a distorted omnidirectional pattern is observed having good co-to-cross isolation.

Fig. 5.6(a)-(b) show the 3-D radiation patterns for element-1 and element-9 of the proposed antenna at 4.81 GHz and 26.5 GHz, respectively, when one port is excited and the rest of the ports are kept matched terminated. It is observed that a simulated peak gain of 5.3 dBi and 7.49 dBi is obtained at 4.81 GHz and 26.5 GHz, respectively. Interestingly observed that all ports are kept excited, 3-D patterns at 4.81 GHz and 26.5 GHz have omnidirectional patterns with nulls in the endfire direction, shown in Fig. 5.6(c)-(d). It has a peak gain value of 5.1 dBi and 6.2 dBi at the frequency of 4.81 GHz and 26.5 GHz, respectively.

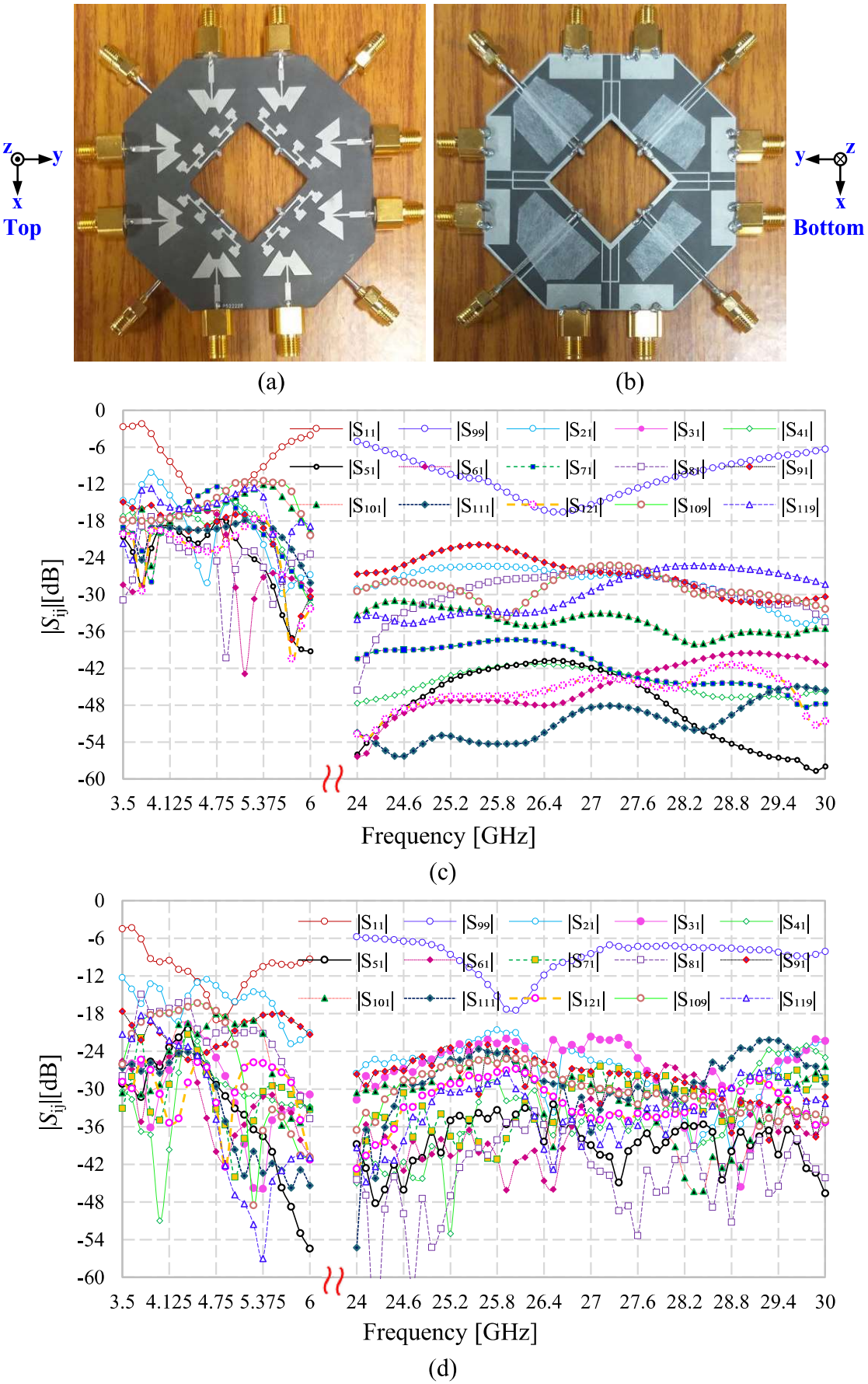

Fig. 5.4: The prototype (a) Top view, (b) bottom view, (c) simulated *S*-parameters, and (d) measured *S*-parameters.

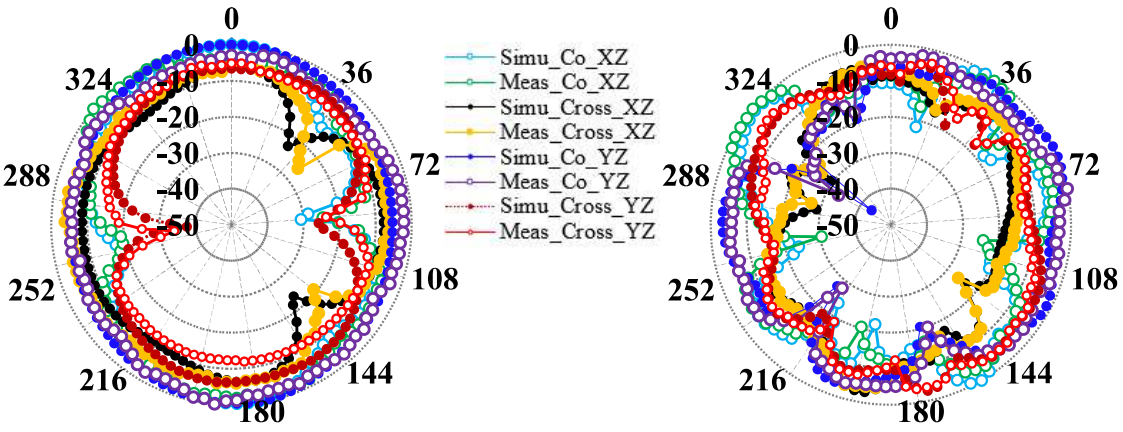

(a) (b)

Fig. 5.5: 2-D radiation patterns in xz- and yz-plane, when one port is excited, and rest all ports are kept matched terminated (a) element-1 at 4.81 GHz, and (b) element-9 at 26.5 GHz.

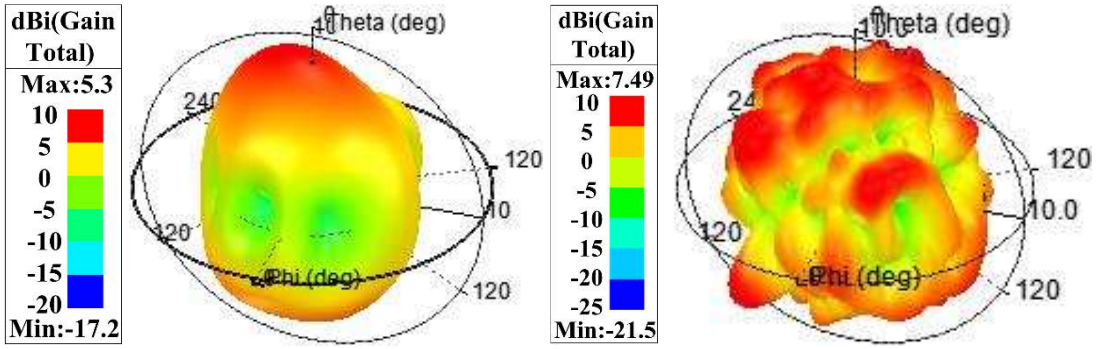

(a) (b)

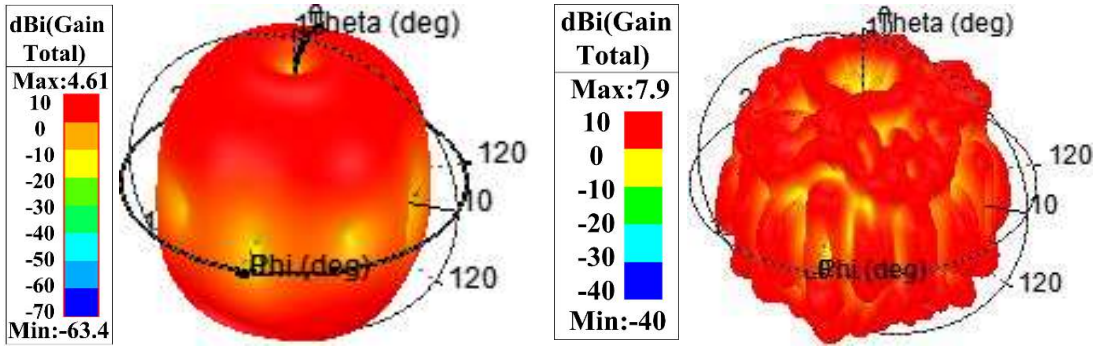

(c) (d)

Fig. 5.6: 3-D radiation patterns, when one port is excited, and rest all ports are kept matched terminated (a) element-1 at 4.81 GHz, (b) element-9 at 26.5 GHz, (c) when all ports are excited at 4.81 GHz, and (d) when all ports are excited at 26.5 GHz.

5.3.3 Gain, Efficiency, and ECC

The total efficiency of the i^{th} element in the N-element MIMO system is approximated in [22]. The values of gain and efficiency for element-1 in the 8-element MIMO antenna is

almost similar to the other elements, i.e., element-2 to -8. Similarly, the plot of element-9 is almost identical to element-10, -11, and -12. Fig. 5.7(a) shows that the gain and efficiency of the proposed antenna rise with the rise in the frequency across the dual frequency band of sub-6 GHz and mm-wave.

To realize the correct behavior of the MIMO antenna, the analysis of envelope correlation coefficient (ECC) is a necessity for practical applications and it is approximated in [27]. A maximum value (simulated using *S*-parameters and 3D-field method and measured using *S*-parameters only) of ECC is 0.2 and 0.025 in the respective dual wideband, as shown in Fig. 5.7(b).

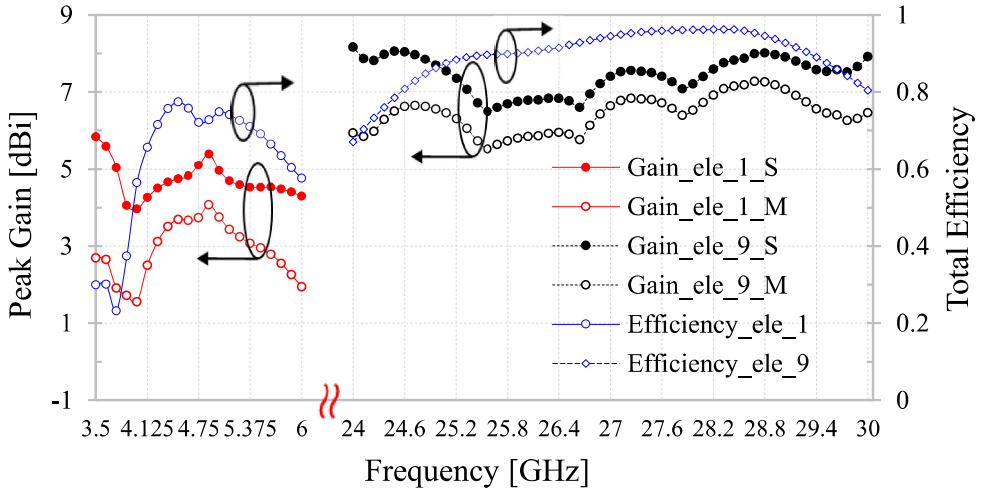

(a)

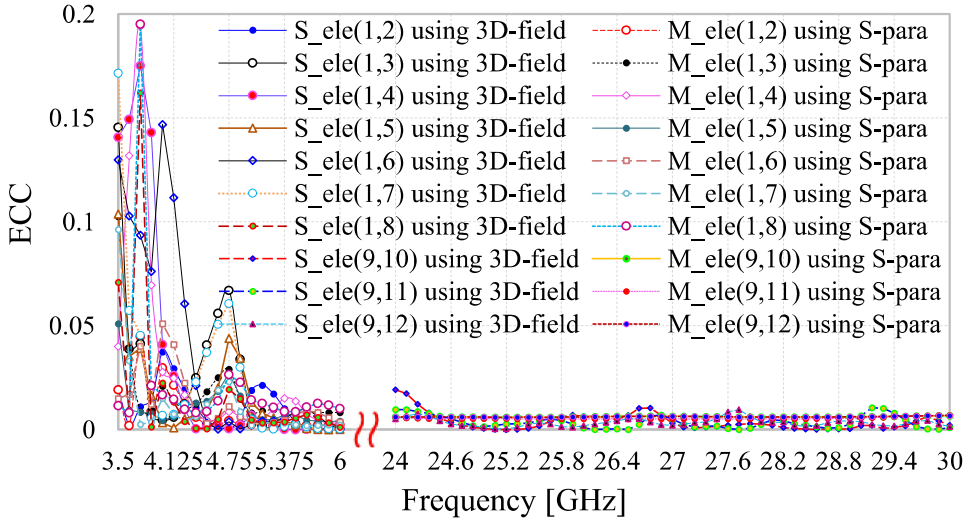

(b)

Fig. 5.7: The proposed MIMO antenna (a) gain and efficiency, and (b) ECC. Abbreviation: S = simulated, M = measured.

5.4 Antenna Integrated within Back Cover

This study investigates an extremely low-profile proposed MIMO antenna integrated inside cavity loaded smartphone's dielectric back cover.

5.4.1 MIMO Antenna with Back Cover

The proposed MIMO antenna is ultra low-profile because its total height is 0.508 mm or about 0.006 λ_0 at 4.0 GHz. The structure of the antenna with smartphone back-cover is illustrated in Fig. 5.8. The material of the back cover is assumed as like polyimide substrate ($\varepsilon_r = 3$, tan δ = 0.002, thickness = 0.75 mm) having a body size of 150×74×4 mm^3 (size of a smartphone). Integrating the antenna inside the back cover's centre creates a cavity of the same size as the antenna substrate board. The occupied area by the MIMO antenna in the dielectric back cover is only 3706.69 mm^2. Therefore, a 0.242 mm thick superstrate will be formed on the top of the antenna, and the bottom of the antenna (ground plane) will be in the same face to the bottom surface of the back cover.

To see the loading effect of the dielectric back-cover on the antenna, the simulated *S*-parameters characteristics are plotted in Fig. 5.9. The slight inconsistency in reflection coefficient ($S_{ij} \in i=j$ < -6 dB) is observed in sub-6 GHz (n79) band, but in mm-wave spectrum frequency shifted towards lower. Still, the mutual coupling ($S_{ij} \in i \neq j$) is almost similar to the free space antenna in the respective dual bands. It still provided a -6 dB impedance bandwidth of 3.8-5.3 GHz ($S_{ij} \in i=j$, *1* to *8*) and 24.0-27.5 GHz ($S_{ij} \in i=j$, *9* to *12*) with a minimum isolation value of -12 dB and -22 dB ($S_{ij} \in i \neq j$, *1* to *12* and *9* to *12*) in the respective spectrum. Fig. 5.10 shows the plots of efficiency and gain for the antenna integrated within the dielectric back cover. It is observed that the efficiency of element-1 and -9 decreases compared to free space antenna in the sub-6 GHz and mm-wave spectrum, respectively. Similarly, the gain of element-1 and -9 improved in the respective

frequency bands. The improvement in the gain occurred mainly due to thick superstrate dielectric loading on that antenna.

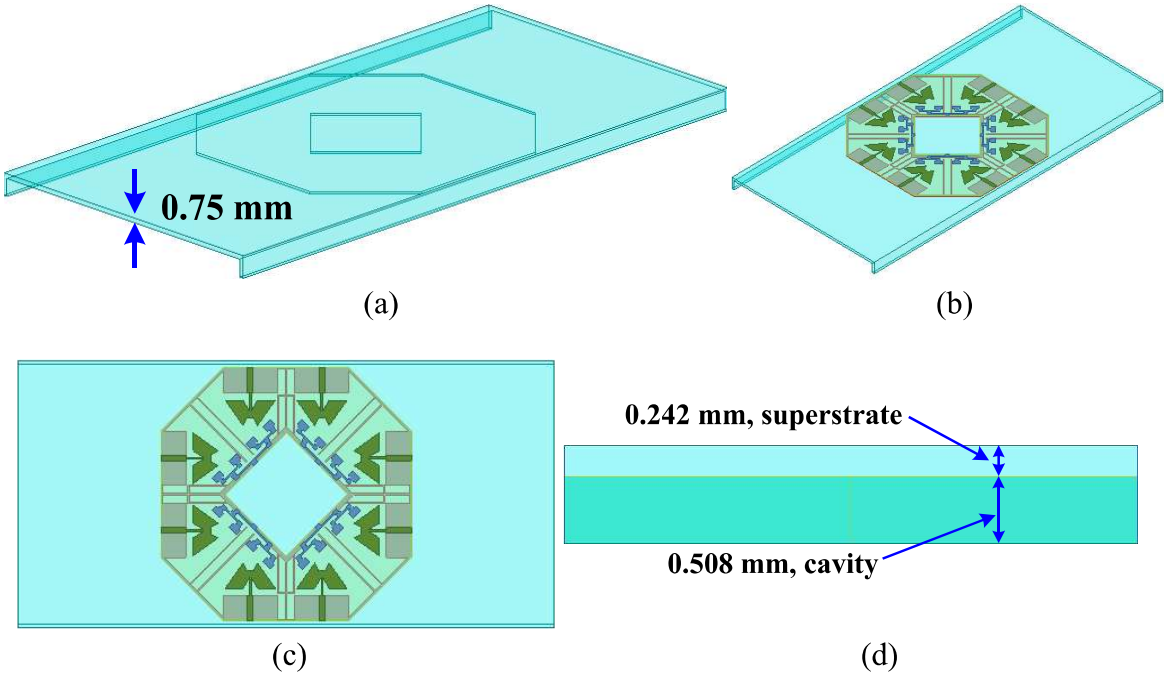

Fig. 5.8: The antenna integrated within dielectric back-cover (a) back-cover's top-side view, (b) top-side view of antenna with back-cover, (c) top view of antenna with back-cover, and (d) side view of back-cover's top.

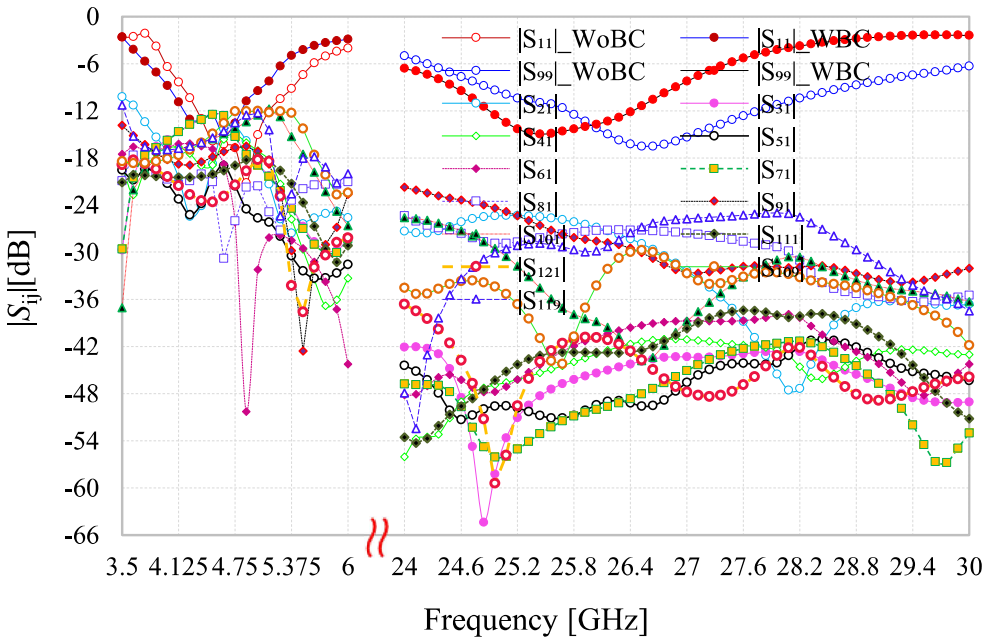

Fig. 5.9: The proposed antenna embedded within a 0.75 mm thick dielectric back-cover corresponding simulated *S*-parameters.
Abbreviation: WoBC and WBC = Without and With Back-Cover.

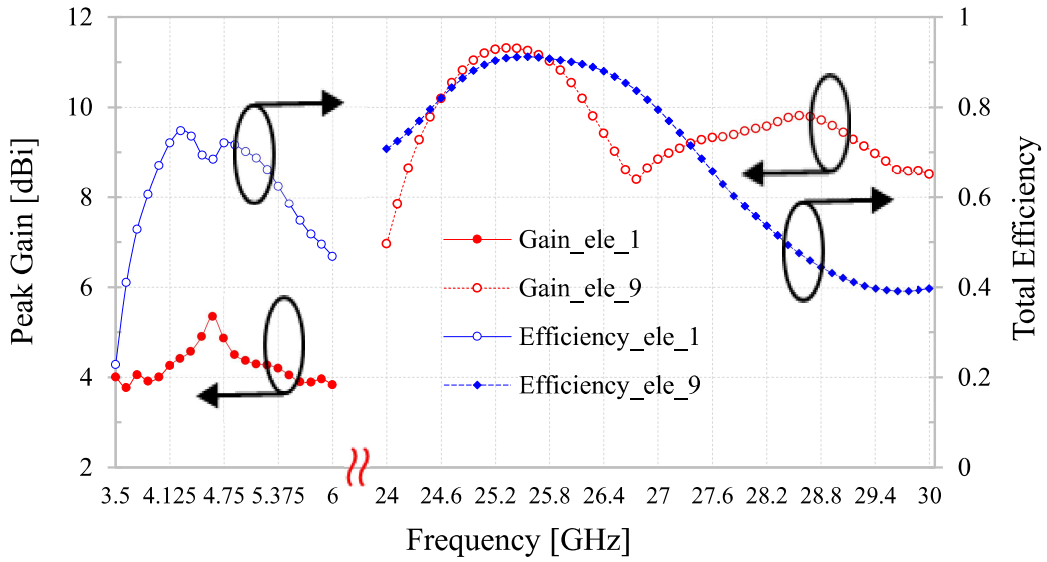

Fig. 5.10: The proposed antenna embedded within a 0.75 mm thick dielectric back-cover corresponding gain and efficiency.

5.4.2 Comparison and Review

To justify the advancement of the antennas performances, the proposed MIMO system is compared with the recently published antenna of the 5G-MIMO antenna integrated with smartphone back-cover, as listed in Table 5.1. All antenna reported in the table cover only 5G sub-6 GHz spectrum, but they are not sufficient for 5G mm-wave coverage and have a much larger profile than the proposed structure. Only design in [112] has a minor total antenna volume. Still, it occupied a lesser area of the smartphone back-cover but suffered from fewer antenna elements and low isolation value. The design scheme in [151] has a minimum coupling and occupies a lesser back-cover area. Still, it has a higher profile and also suffered from the design complexity of the front side module because it used the differential feed technique. The design structure used in [152] has a two-layer with a 100% occupied back-cover area, increasing the fabrication complexity. Based on the data, the proposed MIMO system is suitable to overcome those discussed issues in the reported antennas. The proposed MIMO configuration approach may be a highly suitable candidate for 5G smartphones without occupying the inner space.

Table 5.1: Comparison between the proposed antenna and some reported 5G-MIMO antenna on the back-cover

Ref.	**M_{AE}**	**A_V** ($L\lambda_0 \times W\lambda_0 \times h\lambda_0 \cong LWh \times 10^{-3}\lambda_0^3$)	**IBW [-6dB]** (sub-6 GHz)	**IBW [-6dB]** (mm-wave)	**A_P** (mm)	**I_{min}** (dB)	**P_{DBC}** (mm^3)	**BC_A** (%)	**P_{DMA}** ($L \times W \times h = mm^3$)
[112]	4	0.462×0.462×0.011 ≅ 2.3478	3.3-4.2	NA	1	9.5	150×70×1.2	16.8	42×42×1
[150]	8	2.2×1.173×0.0115 ≅ 29.795	4.4-5.04	NA	0.787	18	150×80×0.787	100	150×80×0.787
[151]	8	1.048×1.048×0.0174 ≅ 19.227	4.37-5.5	NA	1.2	22	150×72×1.2	48	72×72×1.2
[152]	8	1.586×0.793×0.0109 ≅ 13.837	3.4-3.8	NA	0.97	10	140×70×0.97	100	140×70×0.97
Prop.	8&4	*0.658967×0.0067 ≅ 4.4634	4.0-5.6	24.25-29.25	0.508	12 & 22	150×74×0.75	33.3	*3706.7 ×0.508

Abbreviations: M_{AE} = number of antenna element in MIMO, A_V = total antenna electrical volume, IBW = impedance bandwidth, NA = not applicable, A_P = antenna profile, I_{min} = minimum isolation, P_{DBC} = physical dimension dielectric back-cover, BC_A = occupied back-cover area by antenna, P_{DMA} = physical dimension of MIMO antenna. where $\lambda_0 = c/f_0$ being highest operating wavelength (f_0 in GHz) and * = occupied area.

5.5 Summary

In this chapter, an appropriate high-order 5G-MIMO system is investigated for the smartphone's back-cover by integrating the 5G sub-6 GHz and mm-wave antennas that secure -6 dB 5G NR spectrum band of n79 (33.33%) and n257/n258 (19.53%) with a high isolation value of 12 dB and 22 dB, respectively. Moreover, the values of peak gain and total efficiency for element-1 and element-9 are 5.4 dBi and 8 dBi, and 56.5-77.4% and 70.3-96.2%, respectively, in the respective dual-band. Also, ECC values are <0.2 and <0.025 in the respective dual-band. The obtained satisfactory results confirm that the proposed MIMO antenna is appropriate for integrating within the dielectric back-cover of smartphones to reduce the device's inner volume and secure satisfactory performances. Therefore, the proposed ultra low-profile MIMO antenna may be a highly potential 5G smartphone applicant.

Finally, the contributions, key findings, and concluding remarks of the presented investigation in this thesis are summarized in chapter 6. A glimpse for future research work on the related area is given at the end of the chapter.